Earthquakes and Structures, *Vol. 15, No. 4 (2018) 411-417*
DOI: https://doi.org/10.12989/eas.2018.15.4.411

Vibration mode decomposition response analysis of large floating roof tank isolation considering swing effect

Jiangang Sun[1a], Lifu Cui[*1], Xiang Li[1b], Zhen Wang[1a], Weibing Liu[1b] and Yuan Lv[2c]

[1]*College of Civil Engineering, Dalian Minzu University, Dalian, China*
[2]*Institute of Road and Bridge Engineering, Dalian Maritime University, Dalian, China*

(Received December 10, 2017, Revised June 4, 2018, Accepted July 14, 2018)

Abstract. To solve the seismic response problem of a vertical floating roof tank with base isolation, the floating roof is assumed to experience homogeneous rigid circular plate vibration, where the wave height of the vibration is linearly distributed along the radius, starting from the theory of fluid velocity potential; the potential function of the liquid movement and the corresponding theoretical expression of the base shear, overturning the moment, are then established. According to the equivalent principle of the shear and moment, a simplified mechanical model of a base isolation tank with a swinging effect is established, along with a motion equation of a vertical storage tank isolation system that considers the swinging effect based on the energy principle. At the same time, taking a 150,000 m^3 large-scale storage tank as an example, a numerical analysis of the dampening effect was conducted using a vibration mode decomposition response spectrum method, and a comparative analysis with a simplified mechanical model with no swinging effect was applied.

Keywords: storage tank; swinging; isolation; seismic response

1. Introduction

Earthquake damage to a vertical tank with a floating roof mainly includes the sticking and instability of the roof, elephant's foot buckling, diamond buckling of the tank wall, and destruction of the connecting parts, among other factors (2003, 2017). To reduce the earthquake response of a storage tank, isolation measures of the tank foundation can be applied. Seleemah (2011) investigated the seismic response of elevated broad and slender liquid storage tanks isolated by elastomeric or sliding bearings. Moeindarbari (2014) investigated 60 records for multiple level seismic hazard analysis and have proposed mathematical formulations involving complex time history analysis. Saha (2015, 2016) investigated the correlation between different earthquake intensity measure (IM) parameters and peak response quantities of the base-isolated liquid storage tanks.

When a tank has a seismic and isolation design, the liquid in the tank is generally divided into a rigid pulse quality, liquid-solid coupling quality of the tank wall, and liquid sloshing quality when moving with the tank wall, and only the horizontal motion of the abo e three particles is considered without consideration of swinging effect of the tank. In engineering, however, a storage tank under the action of an earthquake, includes a reservoir, base, foundation, isolation device, and tank together as a system that moves with seismic motion. In addition to horizontal motion, a tank system also generated a swinging effect. In view of this, the present paper takes a large vertical storage tank with base isolation as the research object, and establishes a simplified model that only considers the translation of three types of particles, where no swinging is presented with base isolation motion equations. A motion equation of a vertical tank with base isolation is deduced, which considers the effects of foundation swing on the base. Vertical storage tanks of 150000 m^3 in size were selected, a vibration mode decomposition response spectrum method is used to study a large floating roof tank isolation effect under the action of an earthquake, and a comparative analysis is conducted using a base isolation tank without considering its effect.

2. Basic assumptions

A reservoir is assumed to have ideal fluid irrotationality, and to be inviscid and incompressible. In addition, a floating roof is assumed to be a homogeneous circular plate, the unit area of which is in meters. The isolation device is set at the top of the tank foundation, the upper tank floats on the isolation layer, and the isolation layer can pass the level displacement $x_0(t)$, stiffness k_0, and damping c_0. Considering the influence of foundation swinging, the swinging of the bottom of the storage tank has linear rotation with angle α. The tank wall occurs to flexible deformation in the process of vibration, the displacement changes at $w(\theta,z,t)$, the level incentive of the ground vibration is $\ddot{x}_g(t)$. The geometry coordinates and related parameters of the tank is shown in Fig. 1.

*Corresponding author, Associate Professor
E-mail: fangzaijianzai@163.com
[a]Professor
[b]Postgraduated
[c]Ph.D. Student

http://www.techno-press.com/journals/eas&subpage=7
ISSN: 2092-7614 (Print), 2092-7622 (Online)

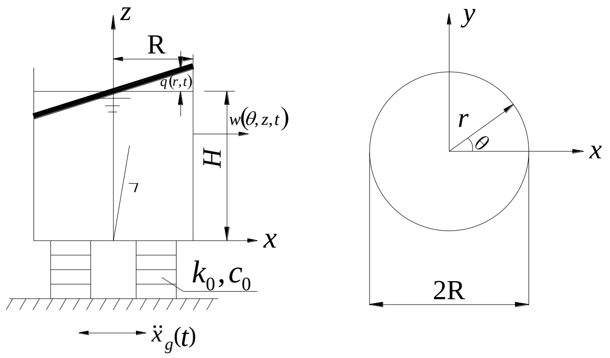

Fig. 1 Geometric coordinate system of tank

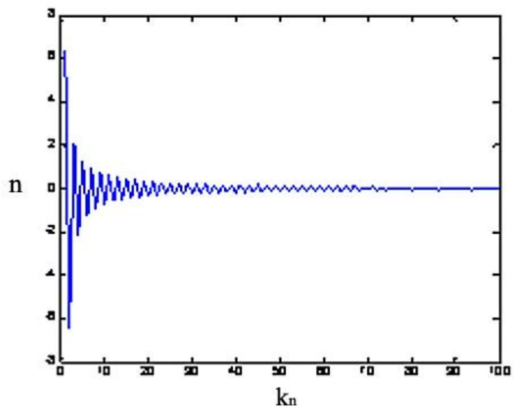

Fig. 2 Variation trend of k_n-n

3. Velocity potential of floating roof tank

Based on the above assumptions and knowledge of the fluid mechanics, the velocity potential $\Phi(r,\theta,z,t)$ of the reservoir fluid should meet the following Laplace equation and boundary conditions

$$\frac{\partial^2\Phi}{\partial r^2}+\frac{1}{r}\frac{\partial\Phi}{\partial r}+\frac{1}{r^2}\frac{\partial^2\Phi}{\partial\theta^2}+\frac{\partial^2\Phi}{\partial z^2}=0 \tag{1}$$

$$\left.\frac{\partial\Phi}{\partial r}\right|_{r=R}=\left[\dot{x}_0(t)+\dot{x}_g(t)+z\dot{\alpha}(t)+\dot{w}(z,t)\right]\cos\theta \tag{2a}$$

$$\left.\frac{\partial\Phi}{\partial Z}\right|_{Z=0}=\dot{\alpha}(t)r\cos\theta \tag{2b}$$

$$\left.\frac{\partial\Phi}{\partial\theta}\right|_{\theta=0,\pi}=0 \tag{2c}$$

$$\left.\frac{\partial\Phi}{\partial z}\right|_{z=H}=\dot{q}(r,\theta,t) \tag{2d}$$

Here, $\dot{x}_g(t)$ is the horizontal earthquake excitation, $\dot{x}_0(t)$ is the relative speed of the isolation layer, $\dot{\alpha}(t)$ is the angular velocity of the foundation swinging, $\dot{w}(z,t)$ is the tank wall radial velocity of the horizontal earthquake excitation direction of the tank wall, and $q(r,\theta,t)$ is the vibration displacement of a floating roof. The velocity potential $\Phi(r,\theta,z,t)$ of a fluid could can be considered the rigid velocity potential φ_1, liquid-solid coupling vibration velocity potential φ_2, and convection shaking velocity potential φ_3, the total velocity potential and can be expressed as

$$\Phi(r,\theta,z,t)=\varphi_1(r,\theta,z,t)+\varphi_2(r,\theta,z,t)+\varphi_3(r,\theta,z,t) \tag{3}$$

3.1 Rigid velocity potential

The horizontal earthquake excitation $\dot{x}_g(t)$ and rigid body motion velocity potential $\varphi_1(r,\theta,z,t)$ of the isolation layer motion $\dot{x}_0(t)$ produced should satisfy the Laplace equation and boundary conditions, namely

$$\varphi_1(r,\theta,z,t)=\left[\dot{x}_0(t)+\dot{x}_g(t)+z\dot{\alpha}(t)\right]r\cos\theta \tag{4}$$

3.2 Liquid-solid coupling velocity potential $\varphi_2(r,\theta,z,t)$

In vertical steel tanks undergoing vibration, to conduct simplified analysis, the tank wall can be simplified into the beam structure. Under the effect of lateral force, the girder structure can only stimulate the girder mode of vibration, and there will be no ring mode of vibration. The velocity potential of elastic deformation $w(z,t)\cos\theta$ produced by the tank should satisfy the Laplace Eq. (1). Using the separation variable method, the boundary conditions (Eq. (2)), the $\varphi_2(r,\theta,z,t)$ is expressed as

$$\varphi_2(r,\theta,z,t)=\dot{w}(t)\cos\theta\sum_{n=1}^{\infty}\frac{2I_1(\lambda_n r)\cos(\lambda_n z)}{H\lambda_n I_1'(\lambda_n R)}k_n \tag{5}$$

Here, $I_1(\lambda_n r)$ is the function of the first type of modified Bessel, and $I_1'(\lambda_n R)$ is the derivative of the first type of modified Bessel function. In addition, H is the height of the reservoir. $\lambda_n=\frac{(2n-1)\pi}{2H}$. $k_n=\frac{H}{\pi}\left[\frac{1}{2n}\left(1-(-1)^n\right)\right]-\frac{H}{\pi}\left[\frac{1}{2(n-1)}\left(1+(-1)^n\right)\right]$. Moreover, k_n is obtained using $w(z,t)=w(t)\sin\frac{\pi z}{2H}$. With the values of n changing, k_n is as shown in Fig. 2, and when the value of n reaches a certain degree, k_n gradually and stably tends toward zero.

The predominant period of an earthquake is smaller than the natural cycle of reservoir shaking under normal circumstances, and when researching convection shaking, the ground motion is thought to have an approximate pulse form, thus ignoring the influence of surface gravity waves. However, when the mid-length cycle of the earthquake spectrum has a significant advantage, the influence of the surface wave cannot be ignored. In addition, the basic cycle of a structure is extended after using a base isolation system, and the influence of the surface wave cannot be ignored at this time; otherwise, a greater error will occur. The convection shaking velocity potential $\varphi_3(r,\theta,z,t)$ is produced through a pressure imbalance under the effects of $\varphi_1(r,\theta,z,t)$ and $\varphi_2(r,\theta,z,t)$, and according to the Laplace equation, when using a separation variable method, the following boundary conditions,

$\varphi_3(r,\theta,z,t)=\sum_{n=1}^{\infty}\dot{q}_n(t)\cosh\left(\sigma_n\frac{z}{R}\right)J_1\left(\sigma_n\frac{r}{R}\right)\cos\theta$ are obtained according to the rigid plate vibration Eq. (4), and expand r to a series form of the first-order Bessel function: $J_1(\sigma_n\frac{r}{R})$.

$$\varphi_3(r,\theta,z,t)=\cos\theta\sum_{n=1}^{\infty}\frac{gb_n}{\omega_n^2}\frac{\cosh\left(\sigma_n\frac{z}{R}\right)}{\cosh\left(\sigma_n\frac{H}{R}\right)}J_1\left(\sigma_n\frac{r}{R}\right)\dot{q}_{cn}(t) \qquad (6)$$

Here, $\omega_n^2=\frac{g}{R}\sigma_n\tanh\left(\sigma_n\frac{H}{R}\right)$, $\dot{q}_{cn}(t)=\left[\dot{\zeta}_0(t)-R\dot{\alpha}(t)\right]$, and $b_n=\frac{2}{(\sigma_n^2-1)J_1(\sigma_n)}$, where σ_n is the root of the first-order Bessel function.

The total velocity potential is

$$\begin{aligned}\Phi(r,\theta,z,t)&=\left[\dot{x}_0(t)+\dot{x}_g(t)+z\dot{\alpha}(t)\right]r\cos\theta\\&+\dot{w}(t)\cos\theta\sum_{n=1}^{\infty}\frac{2I_1(\lambda_n r)\cos(\lambda_n z)}{H\lambda_n I_1'(\lambda_n R)}k_n\\&+\cos\theta\sum_{n=1}^{\infty}\frac{gb_n}{\omega_n^2}\frac{\cosh\left(\sigma_n\frac{z}{R}\right)}{\cosh\left(\sigma_n\frac{H}{R}\right)}J_1\left(\sigma_n\frac{r}{R}\right)\dot{q}_{cn}(t)\end{aligned} \qquad (7)$$

A dynamic fluid pressure at any point in the reservoir is produced through the velocity potential, which meets the linear Bernoulli equation, and thus the dynamic fluid pressure that acts on the tank wall ($r=R$) can be obtained as follows

$$\begin{aligned}P(R,\theta,z,t)&=-\rho_L\left.\frac{\partial\Phi}{\partial t}\right|_{r=R}\\&=-\rho_L\left[\ddot{x}_0(t)+\ddot{x}_g(t)+z\ddot{\alpha}(t)\right]R\cos\theta-\rho_L\ddot{w}(t)\sum_{n=1}^{\infty}\frac{2I_1(\lambda_n R)\cos(\lambda_n z)}{H_w\lambda_n I_1'(\lambda_n R)}k_n\cos\theta\\&-\rho_L\sum_{n=1}^{\infty}\frac{gb_n}{\omega_n^2}\frac{\cosh\left(\sigma_n\frac{z}{R}\right)}{\cosh\left(\sigma_n\frac{H_w}{R}\right)}J_1(\sigma_n)\ddot{q}_{cn}(t)\cos\theta\end{aligned} \qquad (8)$$

The dynamic water pressure acting on a floating top is described as

$$\begin{aligned}P_t(r,\theta,H,t)&=-\rho_L\left.\frac{\partial\Phi}{\partial t}\right|_{z=H}-\rho g q(r,\theta,t)\\&=-\rho_L\left[\ddot{x}_0(t)+\ddot{x}_g(t)+H\ddot{\alpha}(t)\right]r\cos\theta-\rho_L\sum_{n=1}^{\infty}\frac{gb_n}{\omega_n^2}J_1\left(\sigma_n\frac{r}{R}\right)\ddot{q}_{cn}(t)\cos\theta\\&-\rho g(q_{cn}(t)+R\alpha(t))\frac{r}{R}\cos\theta\end{aligned} \qquad (9)$$

The sloshing wave height of a reservoir fluid is

$$q(r,\theta,t)=(q_{cn}(t)+R\alpha(t))\frac{r}{R}\cos\theta \qquad (10)$$

4. Simplified mechanics model and established motion equations

To establish a simplified mechanical model of a floating roof tank isolation analysis, the effect of shear and moment on the tank wall and floor under the action of the outer incentive should first be studied. The shear of the base isolation of a vertical storage tank is applied to the resultant force of the dynamic fluid pressure acting on the tank wall along the height of the tank, which can be determined through an integration of the dynamic fluid pressure of the tank wall

$$\begin{aligned}Q(t)&=\int_0^{H_w}\int_0^{2\pi}R\cos\theta P(R,\theta,z,t)d\theta dz\\&=-\left\{\beta_1\left[\ddot{x}_0(t)+\ddot{x}_g(t)+\frac{H_w}{2}\ddot{\alpha}(t)\right]+\beta_2\ddot{w}(t)+\beta_3\ddot{q}_{cn}(t)\right\}M_L\end{aligned} \qquad (11)$$

The overturning moment that acts on the side panel of a tank wall can be expressed as

$$\begin{aligned}M(t)&=\int_0^{H_w}\int_0^{2\pi}Rz\cos\theta P(R,\theta,z,t)d\theta dz\\&=-\left\{\beta_4\left[(\ddot{x}_0(t)+\ddot{x}_g(t))+\frac{2H}{3}\ddot{\alpha}(t)\right]+\beta_5\ddot{w}(t)+\beta_6\ddot{q}_{cn}(t)\right\}M_L H\end{aligned} \qquad (12)$$

According to the kinetic energy of the reservoir system and the kinetic energy equivalent principle of the equivalent particle, tank wall motion is converted into a liquid-solid coupling particle movement, namely

$$\beta_7 M_L\dot{w}^2(t)=m_f\dot{y}^2(t) \qquad (13)$$

Type: $M_L=\rho_L\pi R^2 H$, $\beta_1=1$,

$$\beta_2=\sum_{n=1}^{\infty}\frac{2I_1(\lambda_n R)\sin(\lambda_n H)}{RH^2\lambda_n^2 I_1'(\lambda_n R)}k_n,$$

$$\beta_3=\sum_{n=1}^{\infty}\frac{gb_n}{\omega_n^2}\frac{\tanh\left(\sigma_n\frac{H}{R}\right)J_1(\sigma_n)}{\sigma_n H},\quad \beta_4=\frac{1}{2},$$

$$\beta_5=\sum_{n=1}^{\infty}\frac{2I_1(\lambda_n R)}{RH^3\lambda_n^2 I_1'(\lambda_n R)}\left[H\sin(\lambda_n H)-\frac{1}{\lambda_n}\right]k_n$$

$$\beta_6=\sum_{n=1}^{\infty}\frac{gb_n}{\omega_n^2}\frac{\tanh\left(\sigma_n\frac{H}{R}\right)J_1(\sigma_n)}{\left(\sigma_n\frac{H_w}{R}\right)R}-\sum_{n=1}^{\infty}\frac{gb_n}{\omega_n^2}\frac{\left(\cosh\left(\sigma_n\frac{H}{R}\right)-1\right)J_1(\sigma_n)}{\left(\sigma_n\frac{H}{R}\right)^2\cosh\left(\sigma_n\frac{H}{R}\right)R},$$

$$\beta_7=\sum_{i=1}^{\infty}\frac{R^2\left[I_0^2(\lambda_n R)-I_1^2(\lambda_n R)\right]-\frac{1}{\lambda_n^2}\left[I_0^2(\lambda_n R)+I_1^2(\lambda_n R)-1\right]}{H_w^2R^2I_1^2(\lambda_n R)}k_n^2.$$

Make $m_r=\beta_1 M_L$, $m_f=\frac{\beta_2^2}{\beta_7}M_L$, $m_c=\beta_3 M_L$, $H_r=\frac{\beta_4}{\beta_1}H$, $H_f=\frac{\beta_5}{\beta_2}H$, and $H_c=\frac{\beta_6}{\beta_3}H$, and make

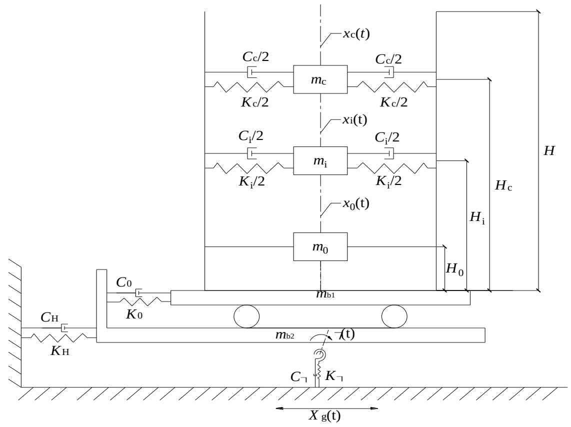

Fig. 3 Mechanical model of floating roof base isolation tank with rotation

the transformations $m_0 = m_r - m_f - m_c$, $H_i = H_f$, $m_0 H_0 = m_r H_r - m_f H_f - m_c H_c$, $\ddot{x}_i(t) = \ddot{y}(t)$, and $\ddot{x}_c(t) = \ddot{q}_{cn}(t)$ owing to the reservoir's rigidity pulse part moving with the tank wall and base. To simplify the calculation, merge the tank's rigid horizontal motion and translation of foundation, ignore the quality of the isolation layer, and further combine the shear and bending moment of the base

$$\begin{aligned} Q(t) = & -m_0\left[\ddot{x}_d(t) + \ddot{x}_g(t) + H_0\ddot{\alpha}(t)\right] \\ & - m_i\left[\ddot{x}_d(t) + \ddot{x}_g(t) + \ddot{x}_i(t) + H_i\ddot{\alpha}(t)\right] \\ & - m_c\left[\ddot{x}_d(t) + \ddot{x}_g(t) + \ddot{x}_c(t) + H_c\ddot{\alpha}(t)\right] \end{aligned} \tag{14}$$

$$\begin{aligned} M(t) = & -m_0 H_0\left[\ddot{x}_d(t) + \ddot{x}_g(t) + H_0\ddot{\alpha}(t)\right] \\ & - m_i H_i\left[\ddot{x}_d(t) + \ddot{x}_g(t) + \ddot{x}_i(t) + H_i\ddot{\alpha}(t)\right] \\ & - m_c H_c\left[\ddot{x}_d(t) + \ddot{x}_g(t) + \ddot{x}_c(t) + H_c\ddot{\alpha}(t)\right] - I_0\ddot{\alpha}(t) \end{aligned} \tag{15}$$

Type: $I_0 = I_r - m_0 H_0^2 - m_f H_f^2 - m_c H_c^2$,

$I_r = \frac{1}{3} M_L H^2$, $x_d = x_0 + x_H$ 。

Eqs. (14) and (15) can be simplified into the mechanical model shown in Fig. 3. An internal liquid is simplified into a three-particle model of convection mass m_c, pulse liquid-solid coupling m_i, and rigid quality m_0. The convection mass and liquid-solid coupling are connected through the equivalent spring and storage tanks, where the equivalent spring stiffness is k_c and k_i, and the damping constant is c_c and c_i, respectively. The rigidity moves with the wall motion of the tank. The foundation is simplified into a rotational spring of stiffness k_α and damping c_α. The rigidity and damping of the isolation device are k_0 and c_0, respectively. In addition, M_{b1} and m_{b2} are respectively the quality of the top and bottom pad beams of the isolation layer. The base sliding displacement, liquid-solid coupling displacement, convection rock displacement, and ground motion displacement are shown using $x_0(t)$, $x_i(t)$, $x_c(t)$, and $x_g(t)$, respectively.

The shaking stiffness is determined based on the vibration equation of the floating roof, shown in Fig. 3, ignoring the influence [4] of the damping term, according to the coordinated relations of the vibration of the floating roof and the liquid sloshing available, namely

$$\ddot{q}_{cn}(t) + \overline{\omega}_n^2 q_{cn}(t) = -\frac{\rho_L R}{\overline{m}}\left[\ddot{x}_0(t) + \ddot{x}_g(t) + H\ddot{\alpha}(t)\right] - \frac{\mathrm{m}R}{\overline{m}}\ddot{\alpha}(t) - \frac{\rho g R}{\overline{m}}\alpha(t) \tag{16}$$

Type: $\overline{m} = m + \rho_L \dfrac{g}{\omega_n^2}$, $\overline{\omega}_n^2 = \dfrac{\rho g}{\overline{m}}$.

Here, k_c is considered based on the floating roof vibration circular frequency, $k_c = \overline{\omega}_n{}^2 m_c$, and the damping ratio of the reservoir can be selected as ξ_c=0.005. Here, k_i is taken from [5]. Moreover, $k_i = \frac{4\pi^5 E h_s m_i}{m}\left[0.000335\left(\frac{H}{R}\right)^3 - 0.000021\left(\frac{H}{R}\right)^2 - 0.016361\left(\frac{H}{R}\right) + 0.065598\right]^2$ where k_0 and c_0 are the stiffness and damping of the isolation layer in Fig. 3, respectively, and the isolation cycle of the engineering design is determined based on an elemental point system. In general, high damping materials are joined in an isolation device, and the damping ratio of the isolation layer may be 0.1 to 0.3.

The ground motion can be simplified into translational and swinging motion, and the level stiffness k_H, damping c_H, rotational stiffness k_α, and damping c_α are determined through [6]

$$k_H = \frac{32(1-\nu_f)G_f R}{(7-8\nu_f)}, \quad c_H = 0.576 k_H R\sqrt{\frac{\rho_f}{G_f}},$$

$$k_\alpha = \frac{8 G_f R^3}{3(1-\nu_f)}, \quad c_\alpha = \frac{0.3 k_\alpha R\sqrt{\rho_f / G_f}}{1 + \dfrac{3(1-\nu_f)I}{8\rho_f R^5}}.$$

Here, ρ_f is the density of the soil; ν_f is the Poisson's ratio of soil; G_f is the shear modulus of the soil, namely, $G_f = \rho_f v_s^2$, where v_s is the equivalent shear wave velocity of the foundation soil; R is the radius of a cylindrical vertical storage tank; and I is the system of the basement mass moment of inertia.

As shown in the mechanical model in Fig. 3, the quality and height of each point change with the change in curve of the tank height–diameter ratio R/H, as shown in Figs. 4 and 5.

Figs. 4 and 5 show that the change in particle parameters is only related to the *D/H*, and when the diameter-height ratio increases, the quality of the sloshing mass point and

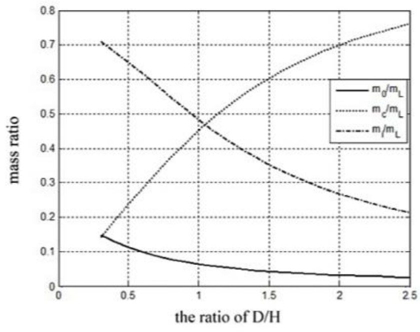

Fig. 4 Quality of each particle varying with the ratio of *D/H*

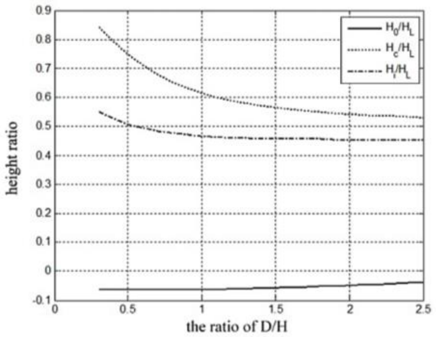

Fig. 5 Equivalent height of each particle varying with the ratio of *D/H*

Table 1 Shear wave velocity of site

Site type	Type I	Type II	Type III	Type IV
Shear wave velocity m/s	650	380	200	100

rigid particles decreases, and the quality of the liquid–solid coupling particles increases. This indicates that when the tank is stout, a short cycle liquid–solid coupling vibration has a dominant role. The inertial effect of the sloshing impact is greater for a slim tank. The height of the equivalent particle is reduced along with the increase in diameter-length ratio, but when the diameter ratio *D/H* is greater than 3.0, the height of the liquid–solid coupling particle shows little change.

Aiming at a simplified mechanical model, when viewing it as a linear isolation system, the corresponding motion equation of the system is obtained using the Hamilton principle.

$$\begin{bmatrix} m_c & 0 & m_c & m_c H_c \\ 0 & m_i & m_i & m_i H_i \\ m_c & m_i & m_c+m_i+m_0 & m_c H_c + m_i H_i + m_0 H_0 \\ m_c H_c & m_i H_i & m_c H_c + m_i H_i + m_0 H_0 & m_c H_c^2 + m_i H_i^2 + m_0 H_0^2 + I_0 \end{bmatrix} \begin{Bmatrix} \ddot{x}_c \\ \ddot{x}_i \\ \ddot{x}_0 \\ \ddot{\alpha} \end{Bmatrix} + \begin{bmatrix} c_c & & & \\ & c_i & & \\ & & c_0 & \\ & & & c_\alpha \end{bmatrix} \begin{Bmatrix} \dot{x}_c \\ \dot{x}_i \\ \dot{x}_0 \\ \dot{\alpha} \end{Bmatrix} + \begin{bmatrix} k_c & & & \\ & k_i & & \\ & & k_0 & \\ & & & k_\alpha \end{bmatrix} \begin{Bmatrix} x_c \\ x_i \\ x_0 \\ \alpha \end{Bmatrix} = - \begin{bmatrix} m_c \\ m_i \\ m_c + m_i + m_0 + m_{b1} \\ m_c H_c + m_i H_i + m_0 H_0 \end{bmatrix} \ddot{x}_g \quad (17)$$

5. Numerical simulation

5.1 Basic parameters

Taking a 150,000 m^3 tank as an example, the isolation effect of a tank was studied. The basic parameters of the 150,000 m^3 tank are as follows: tank diameter D=96.0 m, tank wall height L=22.8 m, reservoir height H=21.0 m, thickness of bottom ring wall plate t_1=40.0 mm, thickness of tank bottom edge plate and T_B=23.0 mm. Japanese produced SPV490 steel was adopted. Considering the base isolation device according to the isolation period T=3 s, the damping ratio of the isolation device is $\xi_0 = 0.1$.

The natural density of the unified foundation soil is 1,700 kg/m^3, where the Poisson's ratio of the soil is v=0.3. The shear wave velocities of different ground soils are listed in Table 1

5.2 Self-vibration characteristics

Using the mass matrix and stiffness matrix of Eq. (17), the natural cycle of the tank structure when considering the characteristic swinging effect is obtained and compared with , which does not consider the natural vibration period of the storage tank with a swinging effect and uses petrochemical steel equipment with the seismic design standard (GB50761-2012, hereafter referred to as the standard GB50761) calculation results.

The Table 2 shows that in the case of different site category, there is little difference in the liquid-solid coupling period between considering the swing impact and not considering the swing impact, and they are also close to the specification values. For the sloshing period, there are differences in the liquid-solid coupling period between considering the swing impact and not considering the swing impact, and the sloshing period considering the swing impact is closer to the specification value. For the isolation period, the sloshing period and liquid-solid coupling period are greater than the those in the non-isolation ones, in the case of four kinds of site categories between considering the swing impact and not considering the swing impact, and it is verified again that the isolation has a magnifying effect on the period of storage tank.

5.3 Seismic response

According to the deduced equation of motion, the damping ratio of liquid sloshing is ξ_1=0.005, and the liquid-solid coupling damping ratio is ξ_2=0.02. Considering

Table 2 Natural vibration period of 150,000 m^3 tank

		Considering the swinging effect [4]				Considering the swinging effect (present study)				
Natural vibration period	Site category	Class I site	Class II site	Class III site	Class IV site	Class I site	Class II site	Class III site	Class IV site	Standard GB50761
The liquid – solid Coupling cycle	No isolation	0.562	0.575	0.621	0.791	0.563	0.575	0.624	0.801	0.557
	Isolation	1.581	1.581	1.581	1.581	1.595	1.596	1.596	1.599	—
Sloshing cycle	No isolation	10.267	10.269	10.278	10.312	12.542	12.543	12.551	12.581	12.547
	Isolation	10.591	10.591	10.591	10.591	12.806	12.806	12.807	12.809	—

Table 3 Calculation results of mode decomposition response spectrum method (considering swinging)

Computational content		Site category	site I	site II	site III	site IV
Ignore swinging impact	Base shear Q (N)	No isolation	2.1973×108	2.7162×108	3.3811×108	3.7221×108
		Isolation	1.3177×108	1.4935×108	1.7942×108	2.2049×108
		Reduction rate %	40.03	45.02	46.93	40.76
	Sloshing wave high h_v (m)	No isolation	1.762	1.762	2.070	2.321
		Isolation	1.792	1.885	2.118	2.378
		Reduction rate %	-1.68	-1.98	-2.33	-2.49
Consider swinging impact	Base shear Q (N)	No isolation	2.1181×108	2.7242×108	5.0891×108	1.1426×109
		Isolation	1.0663×108	1.2611×108	1.6569×108	1.4332×109
		Reduction rate %	49.66	53.71	67.44	-25.43
	Sloshing wave high h_v (m)	No isolation	2.142	2.360	2.689	3.140
		Isolation	2.186	2.421	2.773	3.243
		Reduction rate %	-2.04	-2.56	-3.11	-3.31
Consider and ignore contrastive analysis of swinging effect	Base shear error %	No isolation	3.60	-0.29	-50.52	69.30
		Isolation	19.08	15.56	7.65	35.00
	Sloshing wave high error %	No isolation	-21.57	-33.94	-29.90	-35.29
		Isolation	-21.99	-28.44	-30.93	-36.38

the role of a floating roof under the calculation process, and the interaction of the foundation with the storage tank liquid, the tank and lower soil, in addition to producing a translation during an earthquake, may also cause a swinging of the entire tank; the swinging characteristics and soil types have a direct relationship, namely, the soil movement can be simplified as translational and swinging movements. Taking a 150,000 m^3 tank as an example, MATLAB was used to write a program, and using the mode decomposition response spectrum method, a Jinmen seismic wave (site I), foreign apartment seismic wave (site II), El-centro seismic wave (site III), and Pasadena seismic wave (site IV) were input. Considering a fortification intensity of IX degrees, the seismic peak acceleration takes 0.4 g to reach the base shear and high sloshing wave in the tank under the action of the four types different seismic waves (or sites). The maximum seismic response of the 150,000 m^3 tank is shown in Table 3.

According to the calculation results of the response spectrum method shown in Table 3, considering the base shear of the storage tank under foundation swinging and no foundation swinging, the base shear nearly increases, and no isolation error of site IV reaches 69.3%, and thus when the base shear is calculated, it must be considering a swinging effect. For the sloshing wave height of the liquid, the maximum shaking wave height when considering a swinging impact, as compared with not considering a swinging impact, decreases, and the maximum sloshing wave high of site IV is reduced by 36.38%. This is the same as in, which provides a wave height formula considering the influence of a long period of adjusted response spectrum, which is advised when a tank is designed; the tank swinging should also be considered.

As shown in the analysis results in Table 3, the damping effect of an isolation tank is different under different seismic wave inputs. The base shear damping effect is clear after taking isolation measures, although the control effect of the wave height is poorer, and the wave high effect may even be magnified.

As shown in Table 3, the damping effect of the base shear of a tank on hard ground soil is obviously better than on weak ground soil after taking into consideration the isolation measures. Site I, II, III and IV indicate that the ground soil is from hard to weak. The base shear value on hard ground is less than that of weak ground. This is because when seismic isolation measures are adopted, the liquid-solid coupling period of weak ground is less different than that without seismic isolation. And the liquid-solid coupling period of hard ground is much different than that without seismic isolation. Large periodic difference can effectively avoid structural resonance. The base shear of an isolation tank at sites I, II, and III decrease more than 49.66% compared with the base shear of a non-isolation tank, which is basically equivalent to an earthquake shear force with a seismic intensity of 7–8 degrees. In addition, for a storage tank at site IV, the base shear of the isolation tank when considering the swinging effects increases after isolation is applied. Thus, the isolation effect of a storage tank on hard ground is good, however, the design should apply a reasonable isolation device for a storage tank on soft soil ground to ensure that when a major earthquake occurs the isolation tank maintains the proper level of safety. For a damping effect analysis of the sloshing wave height, the differences in damping effect of isolation tanks on different types of ground soil are not significant. The height of the sloshing wave of a base isolation tank slightly increases compared with the height of the sloshing wave of a non-isolation tank.

6. Conclusions

1) Based on the theory of velocity potential, and considering the foundation soil, structural interaction, and the effect of the tank swing, a seismic response analysis simplifying the mechanical model of the base isolation of a vertical storage tank was established.

2) The liquid–solid coupling cycle clearly increases

compared with a natural vibration period in a non-isolation tank, and liquid sloshing cycle before and after isolation change slightly after base isolation is applied.

3) By means of the seismic decomposition reaction spectrum method, the damping effect of the isolation tank at the site I, II, and III is better than that of the site IV.

Acknowledgements

Financial support was provided by the National Natural Science Foundation of China (Nos. 51078063, 51278089, and 51478090). In addition, independent funding by the central government (DC201502040403) through its funding of scientific research projects is gratefully acknowledged.

References

Cui, L. (2012), “Base isolation and sloshing control of large-scale LNG storage tanks”, Dalian Maritime University, 27-36. (in Chinese)

Hao, J., Sun, J., Liu, Y. *et al*. (2014), “Seismic isolation design of 150000 m3 tank pile foundation”, *Earthq. Eng. Eng. Vib.*, **34**(2), 233-239. (in Chinese)

Haroun, M.A. (1992), “Parametric study of seismic soil- tank interaction. I: horizontal excitation”, *J. Eng. Mech.*, ASCE, **118**(3), 783-797.

Ito, T., Morita, H., Hamada, K., Sugiyama, A., Kawamoto, Y., Ogo, H. and Shirai, E. (2003), “Investigation on bucking behavior of cylindrical liquid storage tanks under seismic excitation: 1st report-Investigation on elephant foot bulge”, *ASME 2003 Pressure Vessels and Piping Conference*, American Society of Mechanical Engineers.

Kapogiannis, I.A. and Spiliopoulos, K.V. (2015), “Performance criteria for liquid storage tanks and piping systems subjected to seismic loading”, *J. Press. Ves. Technol.*, **139**(5), 051801

Moeindarbari, H., Malekzadeh, M. and Taghikhany, T. (2014), “Probabilistic analysis of seismically isolated elevated liquid storage tank using multi-phase friction bearing”, *Earthq. Struct.*, **6**(1), 111-125.

National Standards of the People’s Republic of China (2010), Code for Seismic Design of Buildings, China Architecture and Building Press, Beijing. (in Chinese)

National Standards of the People’s Republic of China (2012), Code for Seismic Design of Petrochemical Steel Facilities, China Planning Press, Beijing. (in Chinese)

Niigata Earthquake Investigation Committee of Civil Society (1966), Investigation Report on the Earthquake in Niigata, Tokyo, Niigata Earthquake Investigation Committee of Civil Society. (in Japanese)

Saha, S.K., Matsagar, V.A. and Jain, A.K. (2015), “Reviewing dynamic analysis of base-isolated cylindrical liquid storage tanks under near-fault earthquakes”, *IES J. Part A: Civil Struct. Eng.*, **8**(1), 41-61.

Saha, S.K., Matsagar, V.A. and Jain, A.K. (2016), “Seismic fragility of base-isolated water storage tanks under non-stationary earthquakes”, *Bull. Earthq. Eng.*, **14**(4), 1153-1175.

Seleemah, A.A. and El-Sharkawy, M. (2011), “Seismic analysis and modeling of isolated elevated liquid storage tanks”, *Earthq. Struct.*, **2**(4), 397-412.

Seleemah, A.A. and El-Sharkawy, M. (2011), “Seismic response of base isolated liquid storage ground tanks”, *Ain Shams Eng. J.*, **2**(1), 33-42.

Sun, J. (2009), *Isolation of Large Vertical Storage Tank-Theory, Method, Test*, Science Press, Beijing. (in Chinese)

Sun, J. (2012), “Study of some problems on dynamic response of stand storage tanks”, Harbin Engineering University. (in Chinese)

Sun, J., Cui, L. and Zheng, J. (2005), “Seismic response of large-scale full capacity LNG storage tanks with base isolation”, *J. Harbin Inst. Technol.*, **37**(5), 649-651. (in Chinese)

Sun, J., Cui, L., Hao, J. *et al*. (2013), “The simplified mechanical model and the seismic response for isolation tank with floating roof”, *J. Harbin Inst. Technol.*, **45**(10), 118-122. (in Chinese)

Sun, J., Cui, L., Zhang, Y. *et al.* (2010), “Research on seismic responses of storage-tanks considering soil-structure interaction”, *Earthq. Eng. Eng. Vib.*, **3**0(3), 141-146. (in Chinese)

Sun, J., Hao, J. and Wang, Z. (2005), “Research on the calculation of the mode analysis response spectrum of the seismic base isolation steel storage tank”, *J. Harbin Inst. Technol.*, **37**(5), 649-651. (in Chinese)

Sun, J., Wang, X. and Zhao, C. (2010), “Base theory of seismic isolation of the storage tanks”, *J. Harbin Inst. Technol.*, **42**(4), 639-643. (in Chinese)

Sun, Y., Sun, J., Cui, L. *et al.* (2011), “Numerical research on large base isolation vertical storage tanks with floating roof”, *Word Earthq. Eng.*, **27**(3), 121-123. (in Chinese)

KT